ARCHIVES OF METALLURGY AND MATERIALS
Volume 51 2006 Issue 3

M. KUCHARSKI*, P. FIMA*, P. SKRZYNIARZ*, W. PRZEBINDA-STEFANOWA**

SURFACE TENSION AND DENSITY OF Cu-Ag, Cu-In AND Ag-In ALLOYS

NAPIĘCIE POWIERZCHNIOWE I GĘSTOŚĆ STOPÓW Cu-Ag, Cu-In I Ag-In

The sessile drop method has been used to measure density and surface tension of Cu, In and Cu-Ag, Cu-In and Ag-In mixtures. For pure metals (Cu, In) and for Cu-Ag, Ag-In alloys, the negative temperature coefficients of surface tension have been obtained. In case of Cu-In alloys, the temperature coefficients of surface tension take negative or positive values depending on composition. Experimental values of the surface tension of Cu-Ag, Cu-In and Ag-In are compared with those computed from Butler model and a fairly good agreement is observed.

Keywords: Cu-Ag, Cu-In, Ag-In systems; Density; Surface tension; Lead-free solders

Praca prezentuje wyniki pomiarów gęstości i napięcia powierzchniowego czystych metali (Cu, In) oraz stopów podwójnych Cu-Ag, Cu-In oraz Ag-In. Dla czystych metali (Cu, In) oraz dla stopów podwójnych Cu-Ag i Ag-In uzyskano ujemne wartości współczynników temperaturowych napięcia powierzchniowego ($d\sigma/dT$). Natomiast w przypadku stopów Cu-In uzyskano, w zależności od składu, dodatnie lub ujemne wartości współczynników temperaturowych napięcia powierzchniowego. Dla wszystkich badanych stopów uzyskano zadawalającą zgodność pomiędzy wartościami napięcia powierzchniowego obliczonymi z modelu Butlera, a wynikami eksperymentu.

1. Introduction

Cu-Ag-In alloys are regarded as a potentially lead-free solder, which can be used in various fields of technique, especially in electronics. The surface tension of such a solder is a very important parameter. The aim of this project was to determine the surface tension of binaries Cu-Ag, Cu-In, Ag-In and ternary Cu-Ag-In systems. In this paper the surface tension and density of the limiting binary systems are presented. There is a noticeable disagreement among existing data for these limiting binary systems. To reconcile these differences, measurements of the surface tension and density as a function of temperature and composition were performed. The sessile drop method was used for these measurements in conjunction with X-ray radiography and digital X-ray image processing. The experimental data on the surface tension were described with Butler model.

2. Experimental apparatus

The sessile drop technique was used to measure the density and surface tension of liquid pure metals (Cu, In) as well as Cu-Ag, Cu-In and Ag-In alloys. Alumina plate was used as a substrate material. The experimental work was carried out with the apparatus shown in Fig. 1. It consists of furnace with Superkanthal heating elements combined with Exposcop 8000 X-ray radiographic unit. The furnace had two ports closed by quartz windows. They enabled the molten droplet image to be captured with a radiographic unit. The reaction tube was sealed by water-cooled brass caps at both ends. The metal sample on alumina substrate was placed in graphite container with a screwed cap which was then hung in the furnace. After closing the furnace, purified argon was passed through, and after a few hours power was turned on and temperature set up on 573 K. After 12 hours since the furnace was powered, the temperature was increased to the first selected temperature. A sample was kept in this temperature for one hour before the measurements started. The temperature was measured by two Pt-PtRh10 thermocouples situated above and beneath the graphite container.

At every temperature, six pictures of the sample were taken, and the sample was turned by 60 degrees before the next picture was taken. Each picture was taken 20 seconds after the furnace had been switched off.

---

* DEPARTMENT OF METALLURGY OF NON-FERROUS METALS, AGH UNIVERSITY OF SCIENCE AND TECHNOLOGY, 30-059 KRAKÓW, AL. MICKIEWICZA 30, POLAND
** UNIVERSITY OF CHEMICAL TECHNOLOGY AND METALLURGY, 8K1 OHRIDSKI, 1756 SOFIA, BULGARIA

This time was short enough to keep the temperature of the sample fixed, however, thanks to this procedure, the eddy current induced in the drop did not disturb the shape of the sample. Figure 2 shows the X-ray alloy drop image.

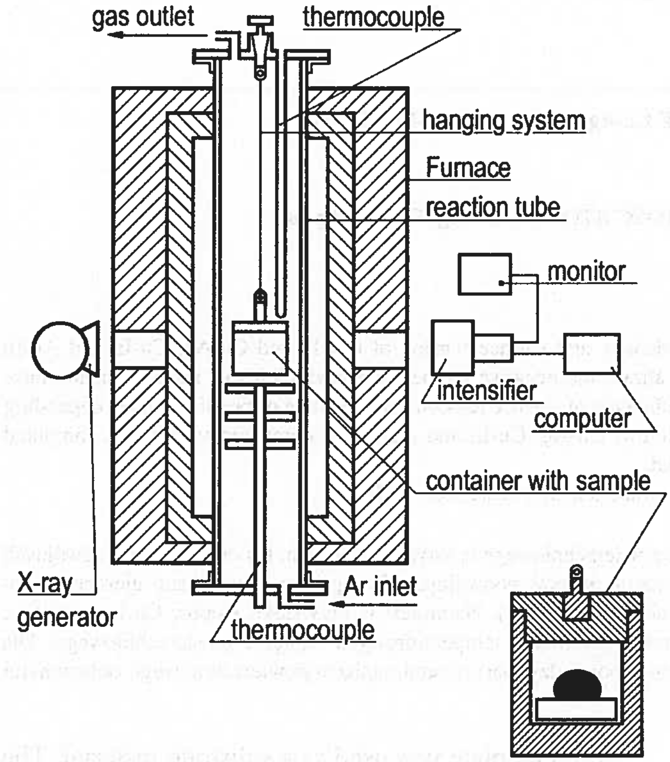

Fig. 1. X-ray radiographic apparatus

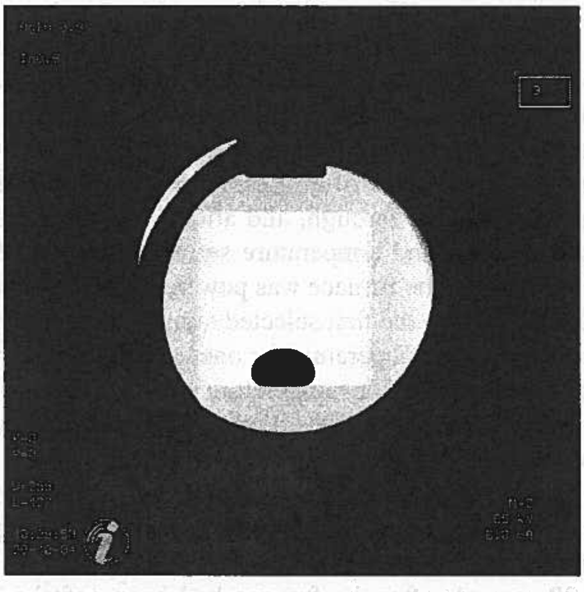

Fig. 2. X-ray image of an alloy drop

After a series of measurements at a selected temperature range, the furnace was turned off, while argon flow was maintained until the furnace reached the room temperature. Using the computer program, coordinates of points on the drop surface were determined. These points were used to calculate density and surface tension of the examined alloys. Surface tension was calculated with the use of computer program based on the method developed by Rotenberg et al. [1]. Their numerical solution of Laplace equation is based on fitting a theoretical Laplacian curve to experimental points. A sum of squared distances from experimental points to the theoretical curve is minimized, and parameters of such a curve representing a solution to the problem are determined.

3. Calibration

The principal requirement of the sessile drop method is to determine the coordinates of the points distributed on the meridian profile of the drop. It will be proved that for the surface tension computations it is not necessary to know the exact dimensions of the sessile drop, however, it is necessary to know it for density measurements. In consequence, the apparatus was calibrated by taking a number of pictures of a steel sphere of known dimensions placed in the furnace at 298–1373 K temperature range. The obtained coordinates of sphere profile were described by a circular curve. The coordinates of the centre of the circle (x_0, z_0) and the radius of the circle (r) were calculated by minimizing the objective function (Q):

$$Q = \sum_{1}^{100} \left[(x_i - x_0)^2 + (z_i - z_0)^2 - r^2 \right]^2 , \qquad (1)$$

where: x_i, z_i are the coordinates of datum experimental point on the circle. Results of the calibration measurements are given in Table 1.

TABLE 1

Results of the calibration measurements

Temperature, K	Sphere diameter, cm	Image diameter, cm	Enlargement coefficient
298	0.6340	1.3842	2.183
573	0.6363*	1.3899	2.184
873	0.6388*	1.3934	2.181
1173	0.6413*	1.4005	2.184
1373	0.6430*	1.4052	2.185

(*) Calculated with coefficient of temperature expansion for steel $\alpha = 13.22 \times 10^{-6}$ [1/K]

Very small variation of the enlargement coefficient suggests excellently stable work of the X-ray apparatus. However, a close inspection of the experimental points' distribution around the determined circle showed that the sphere image was not a circle but an ellipse, as can be seen in Fig. 3. The distortion of the circle coordinates is probably caused by the lack of parallelism between the plane of the sphere and the plane of the intensifier matrix. In order to take into account this distortion a new objective function was formulated:

$$Q = \sum_{1}^{100} \left[\alpha^2 (x_i - x_0)^2 + (z_i - z_0)^2 - r^2\right]^2, \qquad (2)$$

where: α – is distortion coefficient.

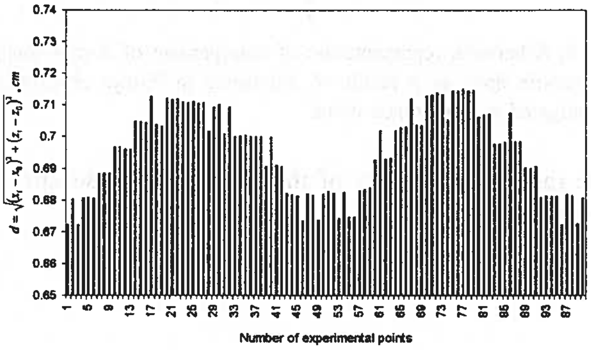

Fig. 3. Distribution of the distances between experimental points (x_i, z_i) and the center of the circle (x_0, z_0)

By minimizing the objective function, new coordinates of the sphere image center (x_0, z_0) and its diameter were calculated as well as the distortion coefficient. The results of the minimization procedure are presented in Table 2.

TABLE 2
Results of the calibration measurements with assumed distortion of x coordinates

Temperature, K	Sphere diameter, [cm]	Image diameter, [cm]	Enlargement coefficient	Distortion coefficient
298	0.6340	1.4201	2.340	1.0257
573	0.6363*	1.4247	2.239	1.0252
873	0.6388*	1.4289	2.237	1.0257
1173	0.6413*	1.4357	2.239	1.0252
1373	0.6430*	1.4408	2.241	1.0256

(*) Calculated with coefficient of temperature expansion for steel $\alpha = 13.22 \times 10^{-6}$ [1/K]

After implementation of the distortion coefficient, the distances between the image centre and the points on the interface profile are distributed more smoothly (Fig. 4).

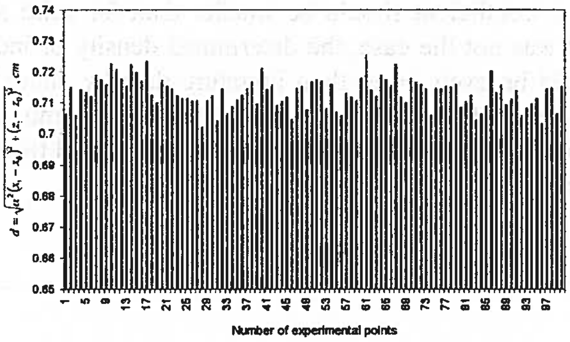

Fig. 4. Distribution of the distances between experimental points (x_i, z_i) and the center of the circle (x_0, z_0) in the case when the distortion coefficient was used

4. Effects of the differences between X-rays absorption by metals

Density results for indium obtained in this work (see Fig. 5) and to a lesser extent for other pure metals [2] suggest that a systematic error may have been involved in our measurements.

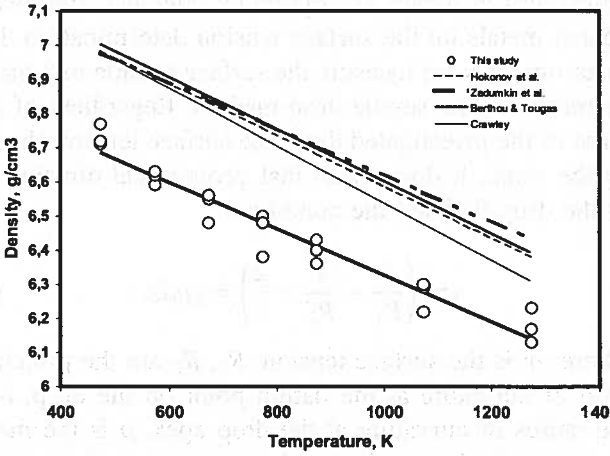

Fig. 5. Density of indium versus temperature

Figure 5 illustrates measured density of indium in comparison with literature data [3–9]. It is easy to notice that our results for density are consistently lower by 4-5% than the data reported in literature. The analysis of these results may suggest that the difference between X-rays absorption by steel and investigated metals would give such results. If investigated metal absorbs X-rays more than steel, determined volume of the metal drop is higher than the real one. In consequence, determined density is lower than should be. To prove this hypothesis, the cylinders were manufactured from pure metals (Cu, Ag, Sn, Bi, In) of which X-rays images were taken. The results are enclosed in Table 3.

The results for indium and other pure metals confirmed our hypothesis, and suggest that for liquid indium the α coefficient should be smaller than for solid state. If it was not the case, the determined density of indium would be even lower than literature data by about 7%. This is confirmed by the values in the last column of the Table 3. The coefficients $\alpha_{(l)}$ can be determined from the relation:

$$\alpha \approx \alpha_{(l)} = \frac{\rho_{literature}}{\rho_{measured}}. \tag{3}$$

TABLE 3
The results of measurements of cylinders made of pure metals

Metal	Mean diameter of image, cm	Mean diameter of cylinder, cm	$\alpha = \left(\frac{d_{image}}{d_{measured}}\right)^2$	α_l
Cu	0.5431	0.5433	1.000	0.997
Ag	0.5462	0.5429	1.012	0.997
Bi	0.5404	0.5312	1.034	0.997
Sn	0.5403	0.5346	1.022	1.015
In	0.5432	0.5247	1.071	1.045

In such a situation we must discuss the impact of the differences in X-rays absorption by reference and investigated metals on the surface tension determination. Let us assume that we measure the surface tension of a metal by means of the sessile drop method. Regardless of the mass of the investigated drop, the surface tension should be the same. It does mean that geometrical dimensions of the drop fulfilled the condition:

$$\sigma d\left(\frac{1}{R_1} + \frac{1}{R_2} - \frac{2}{b}\right) = g\rho dz, \tag{4}$$

where: σ is the surface tension, R_1, R_2 are the principal radii of curvature at the datum point on the drop, b is the radius of curvature at the drop apex, ρ is the metal density, g is the gravitational constant, z is the vertical axis.

In our case, density is determined with some error, therefore the condition (4) can be modified:

$$\sigma d\left(\frac{1}{R_1} + \frac{1}{R_2}\right) = gzd\rho + g\rho dz. \tag{4a}$$

Let us now assume that the obtained dimensions of the drop are higher than they should be as a result of higher absorption of X-rays by the investigated metal in comparison with the reference one. Let dr be the distance of which every point is transferred from a real position to a position on the obtained image. Coordinates of the points on the image (Fig. 6) can be expressed by means of the equations:

$$x' = x + dx = x + dr\sin\varphi \tag{5}$$

$$z' = z + dz = dr + z - dr\cos\varphi = z + dr(1 - \cos\varphi). \tag{6}$$

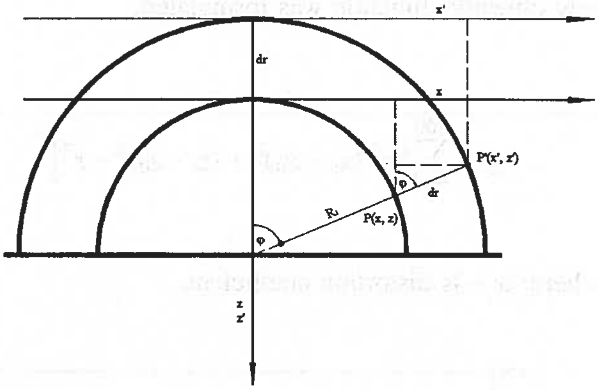

Fig. 6. Schematic representation of enlargement of X-rays image of the sessile drop as a result of difference in X-rays absorption of investigated and reference metal

The radii of curvature of the image of the sessile drop are equal:

$$R_1' = R_1 + dr \tag{7}$$

$$R_2' = \frac{x'}{\sin\varphi} = \frac{x + dr\sin\varphi}{\sin\varphi} = R_2 + dr. \tag{8}$$

For a true image of the sessile drop, the surface tension can be calculated from the equation:

$$\sigma\left(\frac{1}{R_1} + \frac{1}{R_2}\right) = \frac{2\sigma}{b} + \rho gz. \tag{9}$$

Let us assume that the surface tension determined from the larger drop is $\sigma + d\sigma$ instead of σ. Laplace equation for this case is:

$$(\sigma + d\sigma)\left(\frac{1}{R_1 + dr} + \frac{1}{R_2 + dr}\right) = \frac{2(\sigma + d\sigma)}{b + dr} + g(\rho + d\rho)(z + dz), \tag{10}$$

where: $dz = dr(1 - \cos\varphi)$.

The equation (10) can be rewritten to the form:

$$(\sigma + d\sigma)\left[\left(\frac{1}{R_1} + \frac{1}{R_2}\right) + d\left(\frac{1}{R_1} + \frac{1}{R_2}\right)\right] = (\sigma + d\sigma)\left[\frac{2}{b} + d\left(\frac{2}{b}\right)\right] + g(\rho + d\rho)(z + dz). \tag{11}$$

Executing multiplication and omitting products with two derivatives Eq. (11) takes the form:

$$\sigma\left(\frac{1}{R_1}+\frac{1}{R_2}\right)+\sigma d\left(\frac{1}{R_1}+\frac{1}{R_2}\right)+d\sigma\left(\frac{1}{R_1}+\frac{1}{R_2}\right)= \\ \frac{2\sigma}{b}+\sigma d\left(\frac{2}{b}\right)+d\sigma\left(\frac{2}{b}\right)+g\rho z+gzd\rho+g\rho dz. \tag{12}$$

Combining Eq. (9) with Eq. (12) and rearranging yields:

$$\sigma d\left(\frac{1}{R_1}+\frac{1}{R_2}-\frac{2}{b}\right)+d\sigma\left(\frac{1}{R_1}+\frac{1}{R_2}-\frac{2}{b}\right)=gzd\rho+g\rho dz. \tag{13}$$

With Eq. (4), Eq. (13) takes the form:

$$d\sigma\left(\frac{1}{R_1}+\frac{1}{R_2}-\frac{2}{b}\right)=0. \tag{14}$$

The expression in brackets is always different from zero, and therefore, the solution of Eq. (14) is $d\sigma = 0$. It does mean that the error in determining real dimensions of the sessile drop as a consequence of X-rays absorption difference does not affect the results of the surface tension calculations.

The problem is that the density is measured in the same experiment, and therefore the error in volume determination results in the error in the density of the investigated metal. It can be easily proved that if there is a difference between X-ray absorption of the investigated metal and the reference one, measured density can be expressed by the relation:

$$\rho_{measured}=\rho_{true}\left(1-\frac{dV}{V}\right), \tag{15}$$

where: V is a true volume of the drop of the investigated metal.

If we use measured density instead of the true one in the surface tension computations, the determined surface tension is related to 'true' surface tension by the relation:

$$\frac{\sigma_{calculated}}{\sigma_{true}}=\frac{\rho_{measured}}{\rho_{true}}. \tag{16}$$

Thanks to Eq. (16) we can easily correct our results of the surface tension if more precise density for measured system will be available in future. In other words, a publication on the surface tension measurements with the sessile drop method should comprise the information about density used in the surface tension computations.

5. Results of density and surface tension measurements of Cu and In

Density and surface tension for pure copper and indium were determined with the sessile drop method and results were compared with literature data. For our measurements, metals of high purity (Cu – 99.995% and In – 99.999%) were used.

Figures 7 and 8 illustrate measured density and surface tension of copper in comparison with literature data. It is easy to notice that our results are in good agreement with the values presented by other authors [10–18].

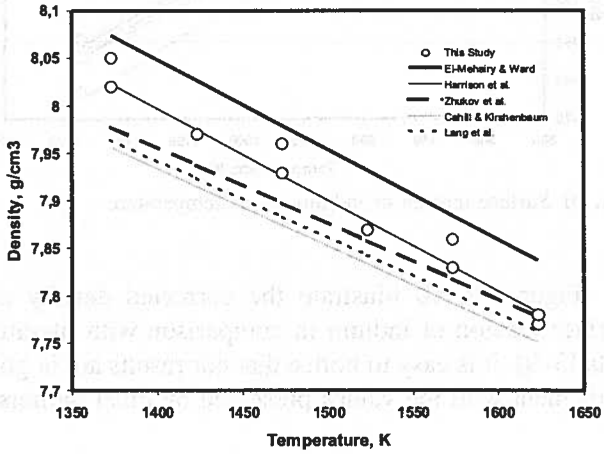

Fig. 7. Density of copper versus temperature

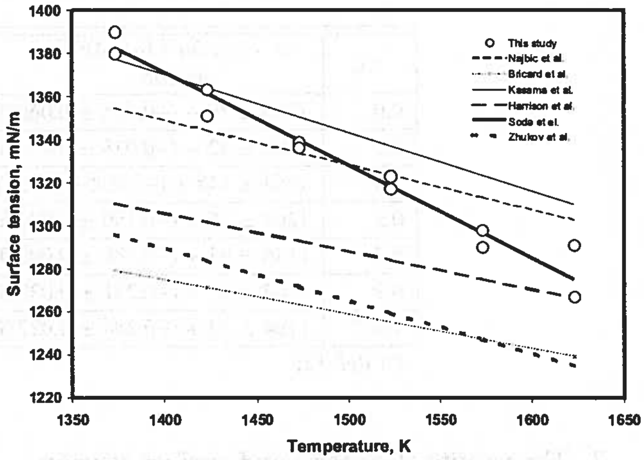

Fig. 8. Surface tension of copper versus temperature

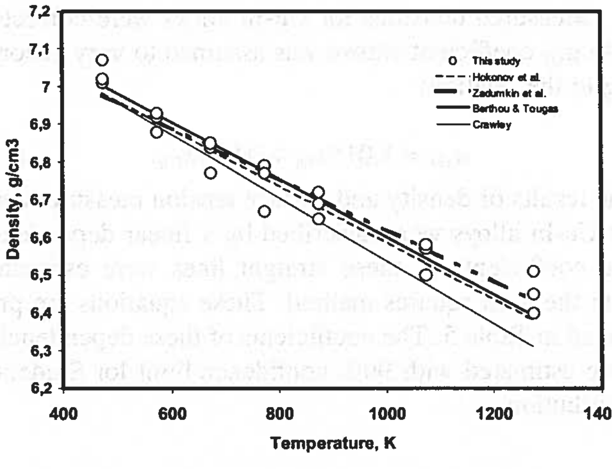

Fig. 9. Corrected density of indium versus temperature

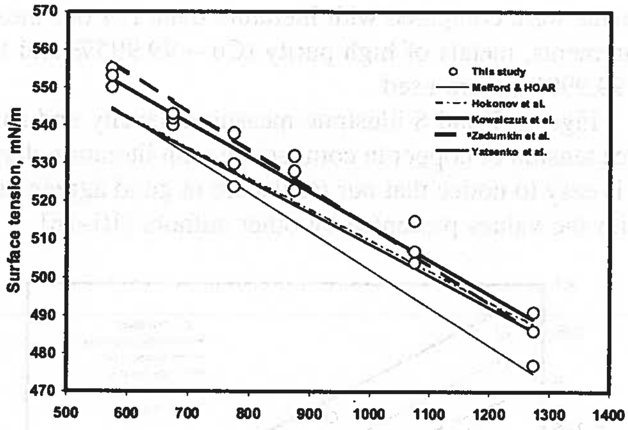

Fig. 10. Surface tension of indium versus temperature

Figures 9, 10 illustrate the corrected density and surface tension of indium in comparison with literature data [3–9]. It is easy to notice that our results are in good agreement with the values presented by other authors.

6. The results of density and surface tension measurements of Cu-Ag alloys

The results of density and surface tension measurements for Cu-Ag alloys were analysed with the least squares method and the obtained linear equations are presented in Table 4. The coefficients of these linear dependencies were estimated with 90% confidence limit for Student's distribution.

For all the investigated Cu-Ag alloys, the surface tension and density decrease with the increase of temperature. Measured values of surface tension for Cu-Ag alloys are higher than the data reported by other investigators [11, 15, 19] for silver-rich alloys, and are in a relatively good agreement with their data for copper-rich alloys. Our data for this system are in accordance with the values reported by Krauze et al. [20] over the whole concentration range. Molar volume of Cu-Ag alloys shows an additive behaviour over the whole concentration range.

TABLE 4

Surface tension (mN/m) and density (g/cm^3) of Cu-Ag alloys

x_{Ag}	$\sigma = a \pm \Delta a + (b \pm \Delta b)T$ mN/m	$\rho = a \pm \Delta a + (b \pm \Delta b)T$ g/cm^3
0.0	1965 ± 76 + (−0.425 ± 0.060)T	9.405 ± 0.156 + (−0.00100 ± 0.00012)T
0.1	1293 ± 42 + (−0.078 ± 0.033)T	9.217 ± 0.429 + (−0.00080 ± 0.00034)T
0.3	1164 ± 148 + (−0.092 ± 0.123)T	9.146 ± 0.246 + (−0.00057 ± 0.00020)T
0.5	1203 ± 35 + (−0.150 ± 0.037)T	9.786 ± 0.153 + (−0.00087 ± 0.00015)T
0.7	1146 ± 93 + (−0.138 ± 0.090)T	10.165 ± 0.038 + (−0.00092 ± 0.00003)T
0.9	1262 ± 37 + (−0.231 ± 0.033)T	11.103 ± 0.330 + (−0.00145 ± 0.00029)T
1.0(*)	1164 ± 33 + (−0.204 ± 0.027)T	10.180 ± 0.092 + (−0.00071 ± 0.00008)T

(*) Ref. [2]

7. The results of density and surface tension measurements of Cu-In alloys

Measured densities for Cu-In alloys were corrected with $\alpha_{(l)}$ coefficient whose was assumed to vary according to the relation:

$$\alpha_{(l)} = 1.015 x_{In} + 0.999 x_{Cu}. \tag{17}$$

The results of density and surface tension measurements for Cu-In alloys were described by a linear dependence and coefficients of these straight lines were estimated with the least squares method. These equations are presented in Table 5. The coefficients of these dependencies were estimated with 90% confidence limit for Student's distribution.

The surface tension of Cu-In alloys decreases with the increase of temperature for some compositions (x_{In} = 0.1, 0.7 and 0.9), while for others (x_{In} = 0.3 and 0.5) an opposite tendency is observed. It is likely to occur due to the increase of the component content with a higher surface tension in the surface layer at the expense of the component with a lower surface tension when the temperature is increased [2].

This phenomenon is confirmed by the experimental data for alloy of x_{In} = 0.5 given by Lee et al. [21]. Their experimental data for alloy of x_{In} = 0.7 have $d\sigma/dT < 0$, however, their calculations suggest a positive value of temperature coefficient. The present measurements for Cu-In system are generally in good agreement with the data of Lee et al. [21].

TABLE 5

Surface tension (mN/m) and density (g/cm³) of Cu-In alloys

x_{In}	$\sigma = a \pm \Delta a + (b \pm \Delta b)T$ mN/m	$\rho = a \pm \Delta a + (b \pm \Delta b)T(^{**})$ g/cm³
0.1	1070 ± 98 + (–0.0635 ± 0.0802)T	8.575 ± 0.315 + (–0.00070 ± 0.00026)T
0.3	674 ± 25 + (0.00800 ± 0.0270)T	8.293 ± 0.176 + (–0.00063 ± 0.00019)T
0.5	535 ± 12 + (0.02347 ± 0.0141)T	8.071 ± 0.337 + (–0.00070 ± 0.00040)T
0.7	598 ± 34 + (–0.0417 ± 0.0401)T	7.639 ± 0.208 + (–0.00064 ± 0.00033)T
0.9	640 ± 23 + (–0.0860 ± 0.0317)T	7.383 ± 0.232 + (–0.00066 ± 0.00031)T
1.0	605 ± 12 + (–0.0930 ± 0.0240)T	7.320 ± 0.098 + (–0.00068 ± 0.00022)T

(**) – corrected

For all the investigated alloys, measured values of density show a linear dependence with the temperature with a negative slope ($d\rho/dT < 0$). Molar volume of Cu-In alloys exhibits an additive relationship despite the large difference between molar volumes of pure copper and indium.

8. The results of density and surface tension measurements of Ag-In alloys

Measured densities for Ag-In alloys were corrected with $\alpha_{(l)}$ coefficient whose was assumed to vary according to the relation:

$$\alpha_{(l)} = 1.015x_{In} + 0.999x_{Ag}. \tag{18}$$

The results of density and surface tension measurements for Ag-In alloys were analysed with least squares method and the obtained equations are enclosed in Table 6. The coefficients of these dependences were estimated with 90% confidence limit for Student's distribution. The surface tension of Ag-In alloys decreases with the temperature increase for all investigated compositions.

Measured surface tension of Ag-In alloys shows an excellent agreement with the data reported by Lee et al. [21]. Molar volume of Ag-In alloys exhibits a positive deviation from additivity. These results are different from the data given by Nakaima [22], who reported a negative deviation of molar volume from additivity for this system.

TABLE 6

Surface tension (mN/m) and density (g/cm³) of Ag-In alloys

x_{Ag}	$\sigma = a \pm \Delta a + (b \pm \Delta b)T$ mN/m	$\rho = a \pm \Delta a + (b \pm \Delta b)T(^{**})$ g/cm³
0.1	618 ± 14 + (–0.089 ± 0.024)T	7.336 ± 0.116 + (–0.00059 ± 0.00023)T
0.3	567 ± 8 + (–0.019 ± 0.012)T	7.875 ± 0.075 + (–0.00075 ± 0.00011)T
0.5	634 ± 18 + (–0.020 ± 0.026)T	8.847 ± 0.189 + (–0.00077 ± 0.00027)T
0.7	808 ± 17 + (–0.071 ± 0.018)T	9.826 ± 0.144 + (–0.00085 ± 0.00015)T
0.9	997 ± 33 + (–0.118 ± 0.029)T	9.754 ± 0.130 + (–0.00078 ± 0.00011)T

(**) – corrected

9. Modelling of the surface tension of A-B binary alloys

Assuming the equilibrium between the bulk phase of A-B alloy and its surface layer which is treated as a true phase, the equation describing the surface tension can be developed [23]:

$$\sigma_{A-B} = \frac{A_A^0}{A_A}\sigma_A + \frac{RT}{A_A}\ln\frac{a_A^{(s)}}{a_A^{(b)}} = \frac{A_B^0}{A_B}\sigma_B + \frac{RT}{A_B}\ln\frac{a_B^{(s)}}{a_B^{(b)}}, \tag{19}$$

where: $a_A^{(s)}$, $a_B^{(s)}$ are the activities of A and B components respectively in the surface layer, $a_A^{(b)}$, $a_B^{(b)}$ are the activities of A and B in the bulk phase of A-B alloy, A_A^0, A_B^0 are molar surfaces of pure component A and pure component B respectively, A_A, A_B are partial molar surfaces of A and B components respectively, R is the gas constant, T is the absolute temperature.

This method was first developed by Butler [24] with the assumption that the difference of composition between the surface phase and the bulk phase is restricted to the first layer of molecules.

The partial excess Gibbs energies of A and B components in bulk phase were described by a polynomial developed by Redlich and Kister [25]:

$$\Delta G_A^{Ex(b)} = x_B^2 \left[L_{AB}^{(0)} + L_{AB}^{(1)}(3x_A - x_B) + L_{AB}^{(2)}(5x_A - x_B)^2(x_A - x_B) + \ldots\right] \tag{20}$$

$$\Delta G_B^{Ex(b)} = x_A^2 \left[L_{AB}^{(0)} + L_{AB}^{(1)}(x_A - 3x_B) + L_{AB}^{(2)}(x_A - 5x_B)^2(x_A - x_B) + \ldots\right] \tag{21}$$

where: $L_{AB}^{(i)} = A_i + B_i T + C_i T \ln(T)$ is a parameter, A_i, B_i, C_i are constants, x_A, x_B are the mole fractions of the solution components.

There is an assumption that the absolute value of partial excess of Gibbs energies of A and B components in the surface layer are smaller than in the bulk because:

– the atom in the surface layer has a lower coordination number than in the bulk phase,

– to reach the surface layer the atom has to acquire more energy than it possesses in the bulk phase.

Therefore, partial excess Gibbs energy of alloy components in the surface layer can be expressed as:

$$\Delta G_A^{Ex(s)} = const \times \left(x_B^{(s)}\right)^2 \left[L_{AB}^{(0)} + L_{AB}^{(1)}(3x_A^{(s)} - x_B^{(s)}) + L_{AB}^{(2)}(5x_A^{(s)} - x_B^{(s)})^2(x_A^{(s)} - x_B^{(s)}) + \ldots.\right] \tag{22}$$

$$\Delta G_B^{Ex(s)} = const \times \left(x_A^{(s)}\right)^2 \left[L_{AB}^{(0)} + L_{AB}^{(1)}(x_A^{(s)} - 3x_B^{(s)}) + L_{AB}^{(2)}(x_A^{(s)} - 5x_B^{(s)})^2(x_A^{(s)} - x_B^{(s)}) + \ldots\right], \tag{23}$$

where: *const* is an adjustable parameter from the range [0–1], $x_A^{(s)}$, $x_B^{(s)}$ are mole fractions of components A and B in the surface layer.

10. Modelling of the surface tension of Cu-Ag, Cu-In and Ag-In alloys

For all the investigated systems experimental data for density suggest that molar volume varies linearly with composition. In consequence, it was assumed that partial molar volumes of copper, silver and indium are equal to molar volumes of respective pure components:

$$V_{Cu} = V_{Cu}^0; \quad V_{Ag} = V_{Ag}^0; \quad V_{In} = V_{In}^0. \tag{24}$$

For calculations, thermodynamic properties of Cu-Ag, Cu-In and Ag-In alloys were described by Redlich-Kister polynomial. The polynomial parameters are summarized in Table 7.

TABLE 7

Redlich-Kister polynomial parameters for Cu-Ag, Cu-In and Ag-In systems

System	Parameters	References
Cu-Ag	$L_{CuAg}^{(0)} = 15171 - 2.537T$ $L_{CuAg}^{(1)} = 2425 - 0.946T$	[26]
Cu-In	$L_{CuIn}^{(0)} = -41564.8 + 238.616T - 29.827T\ln T$ $L_{CuIn}^{(1)} = -76057.8 + 371.306T - 44.994T\ln T$ $L_{CuIn}^{(2)} = -42076.5 + 192.395T - 23.281T\ln T$	[27]
Ag-In	$L_{AgIn}^{(0)} = -14403.297 - 8.176T$ $L_{AgIn}^{(1)} = -15551.028 - 2.664T$ $L_{AgIn}^{(2)} = -710.629 - 5.293T$ $L_{AgIn}^{(3)} = 3955.27$	[28]

Using these values, the surface tension for all these systems was calculated from the model. Experimental data were compared with those computed from the model as can be seen in Fig. 11.

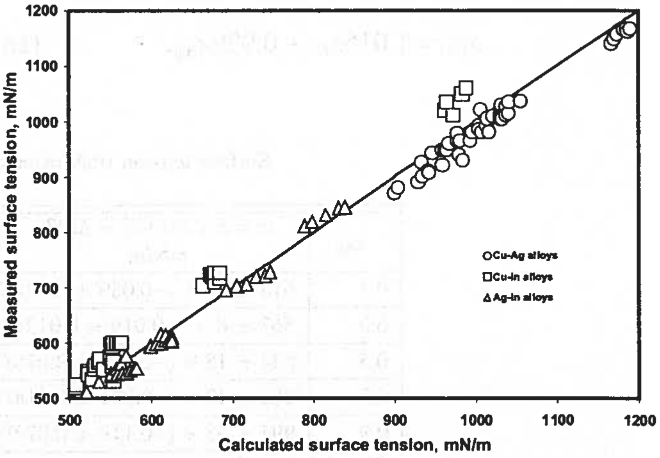

Fig. 11. Comparison of the experimental surface tension of Cu-Ag, Cu-In and Ag-In with those calculated from the model

The surface tension predicted from the model reasonably agrees with the experimental data.

11. Conclusions

Density and surface tension of binaries alloys Cu-Ag, Cu-In, Ag-In were measured with the sessile drop method. Measured densities for pure metals (Cu, In) are in good agreement with the data reported in literature. Density of all the investigated alloys decreases linearly with the increase of temperature.

Surface tension was calculated using a computer program based on Rotenberg et al. [1] method. In case of Cu-In alloys, surface tension decreases linearly with temperature increase for some compositions. For other compositions an opposite tendency is observed ($d\sigma/dT > 0$). This phenomenon is likely to occur if there is a big difference between surface tensions of alloy components. In such a case, according to Gibbs' equation, in the surface layer there is an adsorption of the component with a lower surface tension. Temperature increase causes the increase of concentration of component with higher surface tension in surface layer, which may lead to the increase of alloy's surface tension value.

In case of Cu-Ag and Ag-In alloys surface tension decreases with the increase of temperature for all the examined alloys.

Acknowledgements

The project was financed by the State Committee for Scientific Research in Poland as a part of COST Action 531.

REFERENCES

[1] Y. Rotenberg, L. Boruvka, A.W. Neumann, Journal of Colloid and Interface Science, **931**, May 1983.
[2] M. Kucharski, P. Fima, Monatshefte für Chemie **136**, 1841 (2005).
[3] D.A. Melford, T.P. Hoar, J. Inst. Metals **85**, 197 (1956).
[4] N.B. Hokonov, S.N. Zadumkin, B.B. Alchagirov, Elektokhimja **10**, 911 (1974).
[5] S.P. Yatsenko, V.I. Kononenko, A.L. Suhman, Teplofizika Vysokih Temperatur **10**, 66 (1972).
[6] S.N. Zadumkin, H.I. Ibragimov, D.T. Ozniev, Cvetnaja Metallurgia 82 (1979).
[7] V.F. Kowalczuk, B.A. Kuzniecov, N.P. Kotlovanova, Zhurnal Fiziczeskoj Khimii **42**, 1754 (1968).
[8] A.F. Crawley, Trans. TMS-AIME **242**, 2237 (1968).
[9] P.-E. Berthou, R. Tougas, Metall. Trans. **1**, 2978 October (1970).
[10] Ju.W. Najbic, W.N. Jeremenko, W.W. Fesenko, M.I. Wasilju, L.F. Kirchenko, Powierchnostnyje javlienia w mietallach i splavach i ich rol w processach proskovoj mietallurgii, Izdatjelstvo Akademii Nauk Ukrainskoj CCP, 62 Kijev (1961).
[11] A. Bricard, N. Eustathopoulos, J.-C. Joud, P. Desre, Compt.Rend. **276C**, 1613 (1973).
[12] A. Kasama, A. McLean, W.A. Miller, Can. Metall. Q. **19**, 399 (1981).
[13] D.A. Harrison, D. Yan, S. Blairs, J. Chem. Thermodynamics **9**, 1111 (1977).
[14] H. Soda, A. McLean, W.A. Miller, Trans. JIM **18**, 445 (1977).
[15] A.A. Zhukov, W.N. Kozhurkov, S.I. Popel, O.W. Demidowich, Fiziko-khimicheskie Isledovanja Mietallurgicheskih Procesov, 71, Izdanije UPI Swierdlosk (1979).
[16] A.E. El-Mehairy, R.G. Ward, Trans. Metall. Soc. AIME **227**, 1226 (1963).
[17] J.A. Cahill, A. D. Kirshenbaum, J. Phys. Chem. **66**, 1080 (1961).
[18] G. Lang, P. Laty, J.-C. Joud, P. Desré, Z. Metallkde **68**, 113 (1977).
[19] J. Lee, T. Tanaka, Y. Asano, S. Hara, Materials Transactions, J. Inst. Metals **45**(8), 2719 (2005).
[20] W. Krause, F. Sauerwald, M. Michalke, Z. allgem. Chem. **181** (after [19]), 353 (1929).
[21] J. Lee, W. Shimoda, T. Tanaka, Meas. Sci. Technol. **16**, 438 (2005).
[22] H. Nakajima, Trans. JIM **15**, 301 (1974).
[23] Z. Moser, M. Kucharski, J. Non-Crystalline Solids **156-158**, 369 (1993).
[24] J.A.V. Butler, Proc. Roy. Soc. A **135**, 348 (1935).
[25] O. Redlich, A.T. Kister, Ind. Eng. Chem. **40**, 345 (1948).
[26] P.R. Subramanian, J.H. Perepezko, J. Phase Equilibria **14**, 62 (1993).
[27] H.S. Liu, X.J. Liu, C.P. Wang, I. Ohnuma, R. Kainuma, Z.P. Jin, K. Ishida, J.Phase Equilibria **23**, 409 (2002).
[28] R. Picha, J. Vrestal, A. Kroupa, Computer Coupling of Phase Diagrams and Thermochemistry **28**, 141 (2004).

Received: 10 May 2006.